Utilization of Multi-Sink Architectures for Lifetime Maximization in Underwater Sensor Networks

Huseyin Ugur Yildiz
Department of Electrical and Electronics Engineering
TED University
Ankara, Turkey
hugur.yildiz@tedu.edu.tr

***Abstract*—In a typical underwater sensor networks (USNs) application, sensor nodes convey their collected data from the underwater environment to the central sink node. Improperly positioned central sink node causes two problems. First, sensor nodes consume high energy for transmission if the central sink node is located far away from the nodes where the network lifetime can be negatively affected. Second, long transmission links occurred in such a deployment case causes a USN to have high end-to-end delays since acoustic waves are typical carriers used for USNs. These problems can be mitigated by using multi-sink architectures where sensor nodes transmit their collected data to the nearest sink node/nodes. In this work, we propose a mixed integer programming (MIP) model that maximizes USNs lifetime and we investigate the impact of utilizing multi-sink architectures on network lifetime, end-to-end delay, and node energy consumption as compared to utilizing single-sink architectures. We show that single-sink USNs have at most 51% lower lifetimes than multiple-sink USNs. Furthermore, multiple-sink USNs reduce end-to-end delay and node energy consumption of single-sink USNs by at most 51% and 42%, respectively.**

***Index Terms*—underwater sensor networks, multi-sink architecture, network lifetime, end-to-end delay, energy efficiency, mixed integer programming.**

I. Introduction

Underwater Sensor Networks (USNs) have vast oceanographic applications such as pollution monitoring, tactical surveillance, assisted navigating, *etc.* [1]. A typical USN is formed by using numerous sensor nodes as well as a single centralized sink node. Sensor nodes periodically collect data from the underwater environment and forward the data to the centralized sink node.

USN nodes use acoustic (sound) waves for communication due to the fact that electromagnetic waves have high attenuation in underwater. For time-critical USN applications, long transmission distances cause a USN to have high propagation delays due to the slow speed of sound in underwater (1500 m/s – five orders of magnitude slower than electromagnetic waves). In consequence, long propagation delay results in packets to have high end-to-end delays (time required to reach the sink node from the source node).

In single-sink USNs, nodes near to the sink node deplete their battery energies rapidly than the other nodes. Such an unbalanced energy dissipation causes the *energy hole problem*. Since the network lifetime is generally defined as the time until the first node dies, the energy hole problem in a single-sink architecture has a negative impact on the network lifetime. Moreover, the single-sink architecture results in high end-to-end delays since data collected from sensor nodes may need to traverse long underwater paths to reach the sink node. Furthermore, long paths increase the packet drop rates hence reducing the reliability of the network.

Increasing the network lifetime and reducing the end-to-end delay can jointly be achieved if a multi-sink architecture is adopted [2]. In a multi-sink architecture, the USN consists of numerous sink nodes which are deployed on the surface of the water. Sensor nodes transmit their data to the nearest sink nodes. In this way, the network lifetime, end-to-end delay, and energy consumption of nodes can be improved since the usage of long underwater paths is avoided.

The utilization of multi-sink architectures in USNs is growing day-to-day in the literature. Depth-Based Routing (DBR) [3], GEographic and opportunistic routing with Depth Adjustment-based topology control for communication Recovery over void regions (GEDAR) [4], HydroCast [5], and Hop-by-Hop Dynamic Addressing Based (H2-DAB) [6] are some popular routing protocols that use multi-sink architectures. The problem of choosing the number and locations of multi-sinks has been addressed in several works where the authors develop optimization models to determine optimal sink placement strategies. In [7]–[9], authors show that end-to-end delay and energy consumption decrease as the number of sink nodes increases. However, a quantitative analysis on the network lifetime as the number of sinks changes is ignored in these studies. Although the network lifetime is considered as a performance metric in [10], the number of sink nodes is fixed hence the impact of varying the number of sink nodes on the network lifetime is not considered. Nevertheless, harsh channel conditions of the underwater environment (*e.g.*, path loss, packet drops, *etc.*) are not taken into account in most of the works. An optimal deployment scheme for mobile sinks is proposed in [11] without considering the underwater channel conditions. The most similar to our work is presented in [12] where authors develop an optimization model to determine the network lifetime and optimal sink placement strategy for a given set of sink nodes. However, two-dimensional terrestrial sensor networks are studied instead of USNs.

To the best of our knowledge, the impact of varying the number of sinks on the network lifetime when considering

the harsh underwater channel conditions remains unclear in the USNs literature. To fill the gap in the literature, in this study we formulate a mixed integer programming (MIP) model that maximizes both single-sink and multi-sink USNs lifetimes. The proposed MIP model is built on a detailed energy model which captures the harsh conditions of the underwater environment. By solving the MIP model to optimality, we compare the performances of multi-sink USNs and single-sink USNs in terms of network lifetime, end-to-end delay, and average energy consumption, respectively.

II. System Model

A. Underwater Propagation Model

We follow the principles of the underwater acoustic propagation model presented in [13], [14]. According to this model, the transmission loss in link-(i,j) is calculated as

$$\overline{TL_{ij}(f)} = \overline{TL_0} + 10\kappa \log_{10}(d_{ij}) + d_{ij} \times 10^{-3} \times \overline{a(f)}, \quad (1)$$

where $\overline{TL_0} = 30$ dB models the anomaly in the transmission loss, $\kappa = 1.5$ is the spreading factor in practical cases, f is the central operation frequency of underwater sensor nodes (in kHz), and d_{ij} is link distance (in m). $\overline{a(f)}$ denotes the absorption coefficient (in dB/km) which is calculated as

$$\overline{a(f)} = \frac{0.11 f^2}{1+f^2} + \frac{44 f^2}{4100+f^2} + 2.75 \cdot 10^{-4} f^2 + 0.003. \quad (2)$$

Ambient noise has the following approximated power spectral density

$$\overline{N(f)} \approx 50 - 18 \log_{10}(f). \quad (3)$$

The signal-to-noise ratio (SNR) at the receiver is modeled by using the passive sonar equation as

$$\overline{\gamma_{ij}} = \overline{\mathrm{SL}} - \overline{N(f)} - \overline{TL_{ij}(f)}, \quad (4)$$

where $\overline{\mathrm{SL}}$ is the sound source level (*i.e.*, acoustic transmit power – dB re 1μPa) which is calculated as

$$\overline{\mathrm{SL}} = 10 \log_{10} \left(\frac{P_t}{2\pi H I_0} \right). \quad (5)$$

In this equation, $I_0 = 0.67 \times 10^{-18}$, H, and P_t denote the reference intensity, the depth of the ocean (m), and the electrical transmit power (in W), respectively. Using the binary phase shift keying (BPSK) modulation, the bit error rate is defined as

$$p_{ij}^b = \frac{1}{2} - \frac{1}{2} \sqrt{\frac{\gamma_{ij}}{1+\gamma_{ij}}}. \quad (6)$$

B. Network and Energy Models

We consider a three dimensional static USN where N and M represent the set of sensor nodes and the set of sink nodes. We define set A to cover all directed links. Sensor nodes are uniformly distributed within a region of $d_{net} \times d_{net} \times H$ m^3. We assume that any motion caused by water currents is negligibly small. M static sink nodes are deployed at the surface of the ocean forming a grid topology over a square region of $d_{net} \times d_{net}$ m^2. We assume that sink nodes do not have any constraints on the battery energy. Sensor nodes possess the energy dissipation characteristics of the WHOI Micromodem [15]. This modem has the central operation frequency of 25 kHz (*i.e.*, $f = 25$ kHz) and has the data rate of $R_b = 5$ kbps. The electrical transmit power is set to $P_t = 8$ W while the reception power is $P_r = 1$ W. The maximum transmission range of the WHOI Micromodem is set to $R_{max} = 2.5$ km.

The network lifetime (time until the first node dies) is partitioned as rounds where each round lasts $T_R = 100$ s. A single data flow is initiated by sensor nodes with generating a data packet of size 1024 bits (*i.e.*, $L_D = 1024$ bits), conveyed to nearest sink nodes by using multi-hop communication at each round. To successfully terminate the flow transmission, the transmitter node waits for an acknowledgment (ACK) packet of size 64 bits (*i.e.*, $L_A = 64$ bits) from the receiver node. This process continues until the first node exhausts its battery. However, if both data and ACK packets are not successfully received at both the intended nodes, retransmission is required. The expected number of transmissions needed for successfully terminating a flow is calculated as

$$\varphi_{ij} = \frac{1}{p_{ij}^d \times p_{ji}^a}, \quad (7)$$

where $p_{ij}^d = (1-p_{ij}^b)^{L_D}$ and $p_{ji}^a = (1-p_{ji}^b)^{L_A}$ are the success transmission probabilities of data and ACK packets, respectively.

The transmitter node consumes $(L_D/R_b)P_t$ of energy for transmitting a data packet of size L_D. Moreover, the transmitter node consumes $(L_A/R_b)P_r$ of energy for receiving an ACK packet. Considering retransmissions, the total transmission energy cost for a flow can be expressed as

$$E_{ij}^T = [(L_D/R_b)P_t + (L_A/R_b)P_r] \times \varphi_{ij}. \quad (8)$$

The receiver dissipates $(L_D/R_b)P_{rx}$ and $(L_A/R_b)P_{tx}$ of energies for receiving the data packet and transmitting an ACK packet, respectively. The total reception energy cost for a flow (with retransmissions) is calculated as

$$E_{ji}^R = [(L_D/R_b)P_r + (L_A/R_b)P_t] \times \varphi_{ji}. \quad (9)$$

The total delay experienced in link-(i,j) for a single flow is defined as

$$t_{ij}^D = [L_D/R_b + L_A/R_b + 2d_{ij}/c] \times \varphi_{ij}, \quad (10)$$

where $2d_{ij}/c$ is the round-trip propagation delay which occurs due to the transmissions of both data and ACK packets. Moreover, $c = 1.5$ km/s is the nominal speed of sound in underwater.

C. MIP Formulation for Maximizing the Network Lifetime

We present the MIP framework which has the objective of maximizing the network lifetime in (11). The objective function is defined in (11a) where we define N_R to represent the network lifetime as the number of rounds. Since each round lasts T_R seconds, the network lifetime can also be expressed as $N_R \times T_R$ seconds. Decision variables of the MIP framework are listed as follows:

- f_{ij}^k: Total number of flows generated at node-k transferred over link-(i,j) during the network lifetime.
- N_i: Total number of flows collected at the sink node-i.
- a_i: Binary indicator that takes the value 1 if the sink node-i is used.
- E_i: Total energy dissipated by sensor node-i during the network lifetime (in J).
- N_R: Network lifetime in rounds.

The constraints of the MIP model are defined in (11b)–(11p).

$$\text{Maximize } N_R \times T_R \tag{11a}$$

subject to:

$$\sum_{j \in N \cup M} f_{ij}^k - \sum_{j \in N} f_{ji}^k = s_k \times N_R \text{ if } i = k, \quad \forall i, k \in N \tag{11b}$$

$$\sum_{j \in N \cup M} f_{ij}^k - \sum_{j \in N} f_{ji}^k = 0 \text{ if } i \neq k, \quad \forall i, k \in N \tag{11c}$$

$$\sum_{k \in N} \sum_{j \in N} f_{ji}^k = N_i, \ \forall i \in M \tag{11d}$$

$$\sum_{i \in M} N_i = \left(\sum_{k \in N} s_k \right) \times N_R, \tag{11e}$$

$$\sum_{j \in N \cup M} f_{kj}^k = 0, \ \forall k \in M \tag{11f}$$

$$\sum_{k \in N} \sum_{j \in N} f_{ji}^k \leq a_i \times \mathcal{M}, \ \forall i \in M \tag{11g}$$

$$\sum_{i \in M} a_i = \beta, \tag{11h}$$

$$\sum_{k \in N} \left(\sum_{j \in N \cup M} f_{ij}^k t_{ij}^D + \sum_{j \in N} f_{ji}^k t_{ji}^D \right) \leq N_R \times T_R, \quad \forall i \in N \tag{11i}$$

$$\sum_{k \in N} \left(\sum_{j \in N \cup M} f_{ij}^k E_{ij}^T + \sum_{j \in N} f_{ji}^k E_{ji}^R \right) = E_i, \ \forall i \in N \tag{11j}$$

$$E_i \leq \xi, \ \forall i \in N \tag{11k}$$

$$f_{ij}^k = 0 \text{ if } d_{ij} > R_{max} \text{ or } |z_i| < |z_j|, \quad \forall (i,j) \in A, \forall k \in N \tag{11l}$$

$$f_{ij}^k \geq 0, \quad \forall (i,j) \in A, \forall k \in N \tag{11m}$$

$$a_i = \{0, 1\}, \quad \forall i \in M \tag{11n}$$

$$E_i \geq 0, \quad \forall i \in N \tag{11o}$$

$$N_i \geq 0, \quad \forall i \in M \tag{11p}$$

Const. (11b) is the flow conservation constraint at each source node-k. We define s_k to represent the number of created flows at each round. Since we assume that a single flow is generated at each round, we set $s_k = 1$. During the network lifetime, a total number $s_k \times N_R$ flows are generated. Const. (11c) is the flow balance constraint at each relay node-i which is not a source node. Const. (11d) calculates the number of flows collected at the sink node-i (*i.e.*, N_i). Const. (11e) sums up all collected flows obtained at all sink nodes to the number of generated flows by all sensor nodes during the network lifetime. Const. (11f) ensures that sink nodes cannot generate flows. Const. (11g) uses the binary variable, a_i, to determine whether a sink node-i (where $i \in M$) can receive flows or not. Note that, $\mathcal{M}$ is a sufficiently large number. Const. (11h) guarantees that only β number of sink nodes can be used as final destinations for flows. Const. (11i) enforces that the total delay experienced by each sensor node-i to be less than or equal to the network lifetime. In this constraint, t_{ij}^D values have already been calculated in Eq. (12). In Const. (11j), the amount of energy dissipated by each sensor node is calculated. Furthermore, Const. (11k) bounds the total energy consumption of sensor nodes to the initial provided energy (*i.e.*, $\xi = 1$ MJ). Note that, E_{ij}^T and E_{ji}^R values are calculated in Eqs. (8) and (9), respectively. Const. (11l) employs the maximum transmission rage constraint. Moreover, this constraints enforces a depth based routing such that nodes can only transmit flows to other nodes which have lower depths. We use $|z_i|$ to show the absolute depth of the sensor node-i (in m). Eventually, Consts. (11m)–(11p) define the boundaries of the decision variables used in the MIP model.

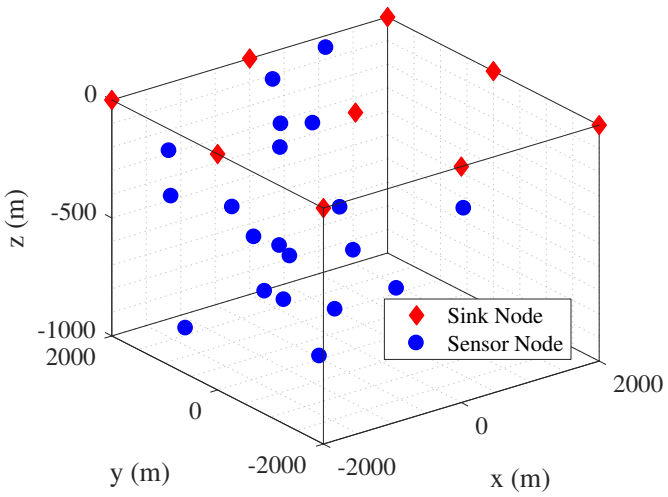

Fig. 1: Randomly generated network topology with 20 sensor nodes and 9 sink nodes where $d_{net} = 4$ km.

III. Analysis

Throughout the experiments, we provide the optimal solutions for the MIP model proposed in (11). Underwater propagation mechanism and energy consumption models are developed in MATLAB while the MIP model is solved by using GAMS/CPLEX 12 solver[1]. The USN that we consider in this work consists of $|N| = 10$, 20, and 30 sensor nodes while the number of sink nodes is taken as $|M| = 9$. We fix

[1]https://www.gams.com/latest/docs/S_CPLEX.html

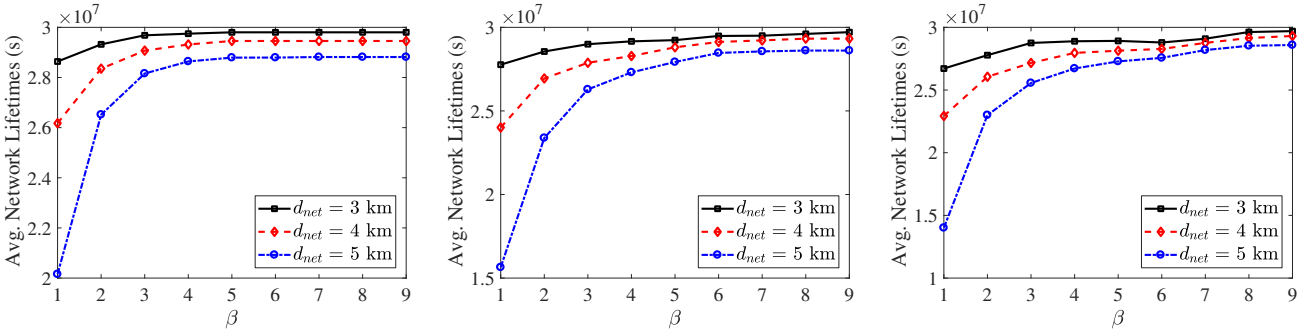

(a) $|N| = 10$ (b) $|N| = 20$ (c) $|N| = 30$

Fig. 2: Average network lifetimes as a function of β for various network configuration options.

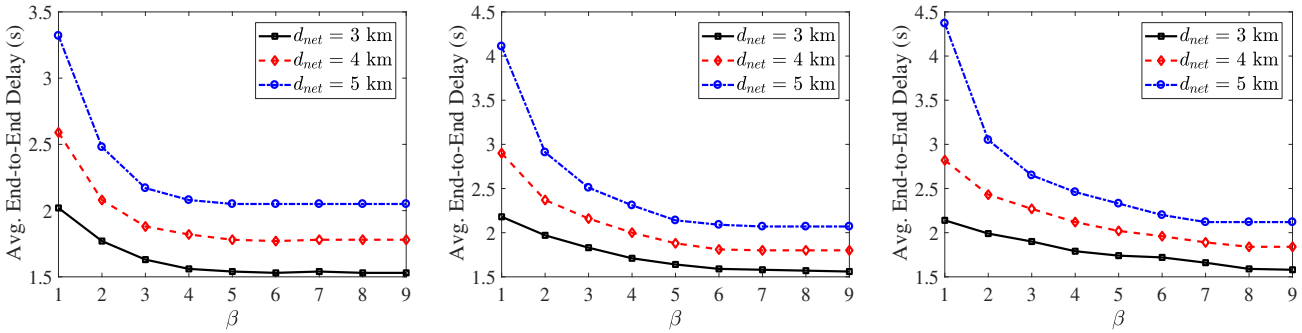

(a) $|N| = 10$ (b) $|N| = 20$ (c) $|N| = 30$

Fig. 3: Average end-to-end delays as a function of β for various network configuration options.

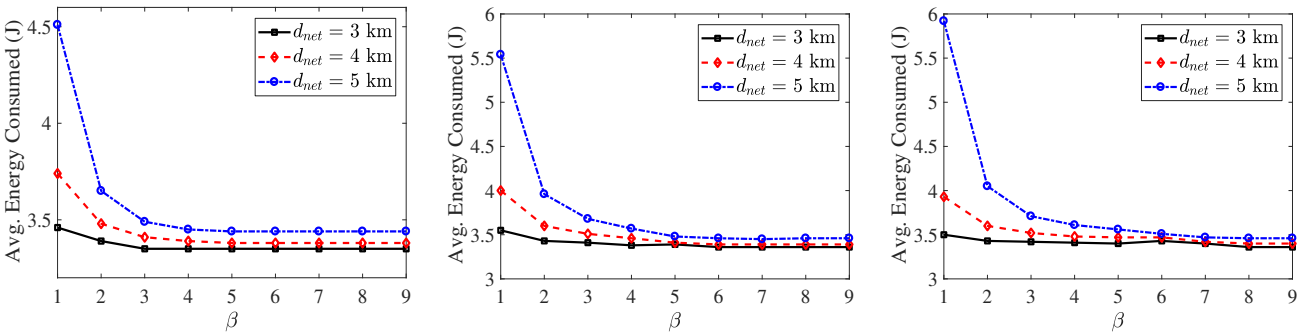

(a) $|N| = 10$ (b) $|N| = 20$ (c) $|N| = 30$

Fig. 4: Average energy consumptions as a function of β for various network configuration options.

the locations of the sink nodes to 3×3 mesh of points spaced $\frac{d_{net}}{2}$ m apart. Edges of the rectangular network area are chosen as d_{net} = 3 km, 4 km, and 5 km. The depth of the water is $H = 1000$ m. β is gradually increased from 1 to 9 ($\beta = 1$ and $\beta > 1$ correspond to single-sink and multi-sink architectures, respectively). We generate 50 random topologies and solve the MIP model for each generated random topology. A randomly generated network topology is given Fig. 1. In this figure, the number of nodes is chosen as $|N| = 20$ where d_{net} is set to 4 km. $|M| = 9$ sink nodes form a 3×3 mesh of points which are separated by 2 km. In the following figures (*i.e.*, Figs. 2–4, we provide the average results obtained for the 50 random topologies. We consider three performance metrics:

1) *Average network lifetime*: We average optimal solutions for $N_R \times T_R$ to present the network lifetimes.
2) *Average end-to-end delay*: We average optimal solutions for f_{ij}^k to calculate the average end-to-end delay as

$$\frac{\sum_{k \in N} \sum_{(i,j) \in A} f_{ij}^k t_{ij}^D}{\sum_{k \in N} \sum_{(i,j) \in A} f_{ij}^k} \tag{12}$$

3) *Average energy consumption per node per round*: We average optimal solutions for E_i to calculate the average energy consumption per node per round as

$$\frac{\sum_{i \in N} E_i}{|N| \times N_R} \tag{13}$$

In Fig. 2, we provide average network lifetimes ($N_R \times T_R$) as a function of the number of sink nodes that can be used as final destinations (*i.e.*, β). We set $|N| = 10$, 20, 30 in Figs. 2a, 2b, and 2c, respectively. Moreover, in each subfigure, we provide our results for the three aforementioned d_{net} values (*i.e.*, $d_{net} = 3$ km, 4 km, and 5 km) to investigate the impact of network density on network lifetimes for a fixed $|N|$.

Average network lifetimes extend as β increases regardless of the network size and density. As an example, in Fig. 2a when $d_{net} = 5$ km, the average network lifetime is obtained as 2.02×10^7 s if a single-sink architecture is utilized ($\beta = 1$). However, as β rises to 9, the average network lifetime extends to 2.88×10^7 s. For a fixed $|N|$, as the network density decreases (high d_{net} values), average network lifetimes decrease since the amount of energy to transmit packets increases as the network gets sparse. Furthermore, for a fixed d_{net}, the increment in $|N|$ yields reduced average network lifetimes. As $|N|$ grows, the number of candidate links for reaching the sink node(s) increases. Hence, the number of hop count also rises which would result in nodes to consume high energy. It is apparent from Fig. 2 that average network lifetimes are highest when $\beta = 9$. Moreover, utilization of a single-sink architecture results in at most 51% lower average network lifetimes as compared to the average network lifetimes obtained for a multi-sink architecture with $\beta = 9$. On the other hand, reducing β from 9 to 5 yields at most 5% lower lifetimes as compared to the lifetimes obtained when $\beta = 9$. This result suggests that deploying a redundant number of sink nodes has a minor impact on prolonging the network lifetime.

In Fig. 3, average end-to-end delays are observed between 1.53 s and 4.37 s. Employing a multi-sink architecture greatly reduces average end-to-end delays of USNs which have a single-sink. For example, in Fig. 3c, the average end-to-end delay is obtained as 4.37 s when $d_{net} = 5$ km for a single-sink deployment. On the other hand, if a multi-sink architecture is adopted (with $\beta = 9$), the average end-to-end delay is dropped to 2.12 s (around 51% reduction). For a fixed $|N|$ as d_{net} grows, long transmission links which increase average end-to-end delays have occurred. When $|N|$ grows for a fixed d_{net}, average end-to-end delays also rise since the number of hop counts to reach the sink node(s) increases. Utilization of only 5 sink nodes reduces the average end-to-end delays of single-sink USNs by at most 47%.

In Fig. 4, each sensor node consumes average energy of 3.35–5.92 J in a single round. Multi-sink architectures have the energy advantage over single-sink architectures. In Fig. 4c, when $d_{net} = 5$ km and $\beta = 1$, we observe that each sensor node consumes an average energy of 5.92 J in each round. However, as we deploy a multi-sink architecture (with $\beta = 9$), the average energy consumption of nodes in a single round reduces to 3.46 J. We also have similar observations as we have in the average end-to-end delay analysis when we vary the network density. In overall, an energy saving at most 42% can be achieved by using a multi-sink architecture rather than a single-sink architecture.

IV. Conclusion

In this work, we quantitatively investigate the effects of utilizing multi-sink architectures over single-sink architectures in USNs in terms of network lifetime, end-to-end delay, and average energy consumption. We propose an MIP model with the objective of maximization of both single-sink and multi-sink USNs lifetime. The MIP model jointly considers the severe conditions of the underwater channel and ensures the reliability of the network via retransmissions. We solve the MIP model to optimality and we show that single-sink USNs have 51% lower network lifetimes than multi-sink USNs. Our results also reveal that multi-sink USNs can reduce the average end-to-end delay and energy consumption of each node (in a single transmission round) by at most 51% and 42%, respectively. Finally, our findings suggest that the utilization of a redundant number of sink nodes has a minor impact to improve the aforementioned network performance metrics.

References

[1] I. F. Akyildiz, D. Pompili, and T. Melodia, "Underwater acoustic sensor networks: research challenges," *Ad Hoc Netw.*, vol. 3, no. 3, pp. 257–279, 2005.

[2] W. K. G. Seah and H. Tan, "Multipath virtual sink architecture for underwater sensor networks," in *Proc. OCEANS - Asia Pacific*, 2006, pp. 1–6.

[3] H. Yan, Z. J. Shi, and J.-H. Cui, "DBR: Depth-based routing for underwater sensor networks," in *Proc. NETWORKING Ad Hoc and Sensor Netw., Wireless Netw., Next Gen. Internet*, 2008, pp. 72–86.

[4] R. W. L. Coutinho, A. Boukerche, L. F. M. Vieira, and A. A. F. Loureiro, "Geographic and opportunistic routing for underwater sensor networks," *IEEE T. Comput.*, vol. 65, no. 2, pp. 548–561, 2016.

[5] Y. Noh, U. Lee, S. Lee, P. Wang, L. F. M. Vieira, J. Cui, M. Gerla, and K. Kim, "HydroCast: Pressure routing for underwater sensor networks," *IEEE T. Veh. Technol.*, vol. 65, no. 1, pp. 333–347, 2016.

[6] M. Ayaz and A. Abdullah, "Hop-by-hop dynamic addressing based (H2-DAB) routing protocol for underwater wireless sensor networks," in *Proc. Int. Conf. on Inform. and Multimedia Technol.*, 2009, pp. 436–441.

[7] S. Ibrahim, J. Cui, and R. Ammar, "Surface-level gateway deployment for underwater sensor networks," in *Proc. IEEE Military Commun. Conf. (MILCOM)*, 2007, pp. 1–7.

[8] S. Ibrahim, J.-H. Cui, and R. Ammar, "Efficient surface gateway deployment for underwater sensor networks," in *Proc. IEEE Symp. on Comput. and Commun.*, 2008, pp. 1177–1182.

[9] S. Ibrahim, M. Al-Bzoor, J. Liu, R. Ammar, S. Rajasekaran, and J. Cui, "General optimization framework for surface gateway deployment problem in underwater sensor networks," *EURASIP J. Wirel. Comm.*, vol. 2013, no. 1, pp. 128:1–13, 2013.

[10] S. Ibrahim, R. Ammar, and J. Cui, "Surface gateway placement strategy for maximizing underwater sensor network lifetime," in *Proc. IEEE Symp. on Comput. and Commun.*, 2010, pp. 342–346.

[11] W. Alsalih, S. Akl, and H. Hassanein, "Placement of multiple mobile data collectors in underwater acoustic sensor networks," in *Proc. IEEE Int. Conf. on Commun.*, 2008, pp. 2113–2118.

[12] W. Hu, C. T. Chou, S. Jha, and N. Bulusu, "Deploying long-lived and cost-effective hybrid sensor networks," *Ad Hoc Netw.*, vol. 4, no. 6, pp. 749 – 767, 2006.

[13] M. Stojanovic, "On the relationship between capacity and distance in an underwater acoustic communication channel," in *Proc. ACM Int. Workshop on Underwater Netw. (WUWNet)*, 2006, pp. 41–47.

[14] J. U. Khan and H. S. Cho, "A data gathering protocol using AUV in underwater sensor networks," in *Proc. OCEANS - TAIPEI*, 2014, pp. 1–6.

[15] L. Freitag, M. Grund, S. Singh, J. Partan, P. Koski, and K. Ball, "The WHOI micro-modem: an acoustic communications and navigation system for multiple platforms," in *Proc. MTS/IEEE OCEANS*, vol. 2, 2005, pp. 1086–1092.